PAPER

Factors affecting the variation of permeability with depth in carbonate aquifers

Stephen R. H. Worthington[1]

Abstract

The permeability of carbonate aquifers varies widely, but the major factors that influence changes in permeability with depth are not well established. Trends in permeability and solute concentration data were analysed for four carbonate aquifers where data were available over a wide range of depths. The Deep Geologic Repository (Ontario, Canada), Edwards Aquifer (Texas, USA), and Chalk aquifer (England, UK) all had permeability data from wells, supplemented by numerical groundwater flow models. There were no permeability data from wells for the fourth site, the Arabika Massif in the Caucasus Mountains (Abkhazia, Georgia). However, the permeability could be calculated from the water-table gradient. It was found that high permeabilities are associated with low solute concentrations, but there is a weak correlation between permeability and depth. The highest permeabilities are found in the freshwater zone, where total dissolved solids (TDS) concentrations are <1,000 mg/L. The presence of aquitards which limit vertical flow were the prime factor in determining the depth of the freshwater zone. This depth varied from 40 m at the Ontario site to >2,000 m below the surface in the Caucasus Mountains. This study highlights the importance of dissolution, the link between permeability and both solute concentrations and flow rate, and how aquitards can play a pivotal role in how permeability varies as a function of depth.

Introduction

Weathering enhances permeability in all bedrock lithologies, but it is particularly important in carbonate aquifers, where dissolution is the main weathering process (Worthington et al. 2016). However, the factors that influence the changes in permeability with depth in carbonates have not been well studied, except in petroleum reservoirs. The study of how permeability varies with depth in the crust has largely focussed on igneous and metamorphic rocks. This is understandable because these lithologies are predominant in the

✉ Stephen R. H. Worthington
    sw@worthingtongroundwater.com

[1] Worthington Groundwater, 55 Mayfair Avenue,
    Dundas, Ontario L9H 3K9, Canada

middle and lower crust (Ingebritsen and Gleeson 2017). Data from thermal and metamorphic heat flow models show that there is a consistent decrease in permeability in at least the uppermost 10–15 km in the crust (Manning and Ingebritsen 1999). Below that depth there is a transition to stresses being accommodated by ductile rather than brittle responses, and there are both fewer data and more uncertainty. Ranjram et al. (2015) compiled permeability measurements from crystalline rocks to a depth of 2,500 m, largely from research projects for nuclear waste repositories. The average trend did show a decrease in permeability with depth, but the correlation was weak ($r^2 = 0.23$), suggesting that multiple factors affect changes in permeability with depth.

Sedimentary rocks predominate in the upper 2 km of the crust, which is also where most permeability measurements have been made (Ingebritsen and Gleeson 2017). Mechanical compaction is an important process in sedimentary rocks, where both porosity and permeability diminish with depth—for instance, a compilation of global data from petroleum reservoirs showed that there are substantial decreases in matrix porosity and permeability with depth due to compaction (Ehrenberg and Nadeau 2005). However, these matrix values

of 10^{-6} to 10^{-7} m/s are several orders of magnitude lower than total hydraulic conductivity values in many carbonate aquifers, although the latter are usually much shallower than petroleum reservoirs.

The principal reason for high permeabilities in carbonate aquifers is that dissolution enhances permeability by enlarging fracture pathways, and the permeabilities of the fracture networks are usually orders of magnitude greater than matrix permeability (Dreybrodt 1990; Worthington and Ford 2009; Kaufmann 2016). Consequently, high permeabilities are likely to occur in carbonate rocks in situations where flow paths enable meteoric water to easily recharge an aquifer, to flow through it, and to discharge from it back to the surface (Stringfield and LeGrand 1966).

The recharge of meteoric water to aquifers not only enhances permeability but also dilutes the solute concentrations of the ambient groundwater. Consequently, this suggests that there may be an inverse correlation between permeability and solute concentrations in carbonate rocks. Domenico (1972) described an upper, intermediate, and lower hydrochemical zone in groundwater, with bicarbonate, sulphate, and chloride, respectively, being the dominant anions in the three zones. Most carbonate rocks were deposited in marine environments, so the original matrix water is typically sea water, with total dissolved solids (TDS) exceeding 30,000 mg/L. If the rocks are interbedded with salt, then TDS in groundwater can increase up to the solubility of halite, 360,000 mg/L. Recharge of meteoric water will ultimately flush out most of the chloride, with sulphate becoming the dominant anion. Gypsum, with a solubility of 2,100 mg/L, is the major source for sulphate. With further flushing most sulphate is removed and bicarbonate becomes the dominant anion. In carbonate aquifers this is derived from dissolution of calcite and dolomite, which have solubilities of 100–500 mg/L, depending on dissolved CO_2 concentrations. A common scheme for classification of water quality is that freshwater has a TDS of <1,000 mg/L, brackish water 1,000–10,000 mg/L, saline water 10,000–100,000 mg/L, and brine >100,000 mg/L (Freeze and Cherry 1979). The anions commonly dominant in these zones are bicarbonate in the freshwater zone, sulphate in the brackish water zone, and chloride in the saline and brine zones (Domenico 1972; Freeze and Cherry 1979). The principal chemical weathering reaction in both silicate and carbonate rocks is dissolution by carbonic acid, and consequently bicarbonate is the principal ion in surface waters that drain from both lithologies (Berner and Berner 2012; Worthington et al. 2016).

Weathering fronts occur where there is a distinct boundary between weathered and unweathered rock (Phillips et al. 2019). The concept of weathering fronts has mostly been applied to silicate rocks, where weathering fronts are usually restricted to depths of metres to tens of metres below the surface (Goldich 1938; Brantley et al. 2013). However,

minerals weather at different rates. Goldich (1938) described the mineral stability series of minerals in igneous rocks, from olivine being the least stable to quartz being the most stable. Consequently, there may be a series of weathering fronts, such as orthoclase, plagioclase, and biotite fronts in granite, and illite, chlorite, calcite, and pyrite fronts in shale (Brantley et al. 2017). There is often an upper weathered layer of saprolite above silicate rocks, dominated by clay minerals and quartz, and a lower fissured layer where weathering along fractures has enhanced the permeability (Lachassagne et al. 2011; Worthington et al. 2016).

Weathering in carbonate rocks is somewhat different because calcite and dolomite dissolve congruently and so leave no residual saprolite layer above the top of intact bedrock. However, weathering (i.e. dissolution) along fractures does produce a high-permeability fissure network, as in granite, although the higher solubility and higher dissolution rates of carbonate minerals result in substantially higher permeabilities than in granite (Worthington et al. 2016). Thermal springs in carbonate aquifers usually have substantially higher sulphate concentrations than nonthermal springs, reflecting the dissolution at depth of sulphate minerals such as gypsum and anhydrite (Worthington and Ford 1995). This suggests that there may be a gypsum front at depth in many carbonate aquifers, above which there are low TDS concentrations and little gypsum or anhydrite present, and below which there are higher TDS concentrations reflecting the dissolution of gypsum and anhydrite. At greater depths there is likely to be a saline front, below which saline ions (Na^{++} and Cl^-) dominate the water chemistry due to the presence of connate water and/ or from the dissolution of halite.

There are two contrasting ways in which carbonate aquifers are usually studied. One is derived from the seminal paper of Hubbert (1940), which Anderson (2008, p. 72) stated that it was "of monumental significance to groundwater theory". A major assumption made by Hubbert is that "the solid framework is insoluble and chemically inert with respect to the fluid flowing through it" (Hubbert 1940, pp. 787–788). Consequently, many modern studies in carbonate aquifers using wells assume that the aquifer rocks are insoluble and that aquifers behave as homogeneous porous media, and so the variation in permeability with depth is not considered. The second way in which carbonate aquifers have been studied focusses on data from caves and springs. These studies often investigate how dissolution enhances permeability, forms caves, and influences spring discharge and chemistry (Ford and Williams 2007; Palmer 2007; Kresic 2013; Stevanović 2015). However, such studies usually do not produce data on permeability, except for individual conduits (e.g. Jeannin 2001), and it would be challenging to quantify changes in permeability with depth from such data. Nevertheless, there have been some studies that have considered the varying permeability with depth in carbonate aquifers.

LeGrand and Stringfield (1971) suggested that the maximum dissolution occurs at approximately the level of the low-flow water table, and decreases exponentially with depth below that level. Milanović (1981) compiled data from voids and high-permeability zones in 146 deep wells in carbonate rocks in Yugoslavia, and inferred that there was an exponential decrease in permeability with depth. Sanford (2017) related depth of flow to permeability up to a depth of 280 m in the steeply dipping Palaeozoic carbonate and siliciclastic rocks in the Valley and Ridge Province in Virginia, USA. Groundwater model calibration showed that there was a much greater permeability reduction with depth than in igneous rocks, which was attributed to a decrease in weathering with depth.

The current study extends the analysis to much greater depths, using data from four contrasting situations. Two approaches are used, with one method being to analyse data from wells, using hydraulic conductivity measurements and modelling results, with solute concentrations giving additional insights into aquifer processes. Three such areas are analysed here, from Canada, the USA, and the UK. The second approach is to utilise data from deep caves that have been mapped down to the water table. The well-documented example of Krubera Cave in the Arabika Massif in Georgia is used. This cave has one of the world's deepest known vadose zones. Although there are no direct measurements of permeability in the aquifer, it was considered to be important to include an example representing the many carbonate aquifers in high mountains where there are deep caves. For instance, Gulden (2020) lists 109 caves in 19 countries that are >1,000 m deep. The data from the four study areas are used to investigate the factors that control changes in permeability with depth below the surface in the four aquifers, as well as the correlation between permeability and solute concentrations.

Study areas

Edwards aquifer, Texas, USA

The Edwards Aquifer in Texas is a Cretaceous limestone 150–250 m thick that underlies San Antonio and provides almost all of the water supply for its 1.7 million residents. It is also widely used for irrigation, and the presence of many wells has facilitated a good understanding of aquifer characteristics such as facies variation, porosity, permeability, and the depth of the potentiometric surface (Hovorka et al. 1996, 1998; Sharp et al. 2019). Several southward-flowing rivers lose much of their flow as they cross the outcrop of the aquifer. Natural discharge occurs from several major springs that are located on faults with substantial displacements, with the flow rising through as much as 200 m of strata that overlie the Edwards Aquifer.
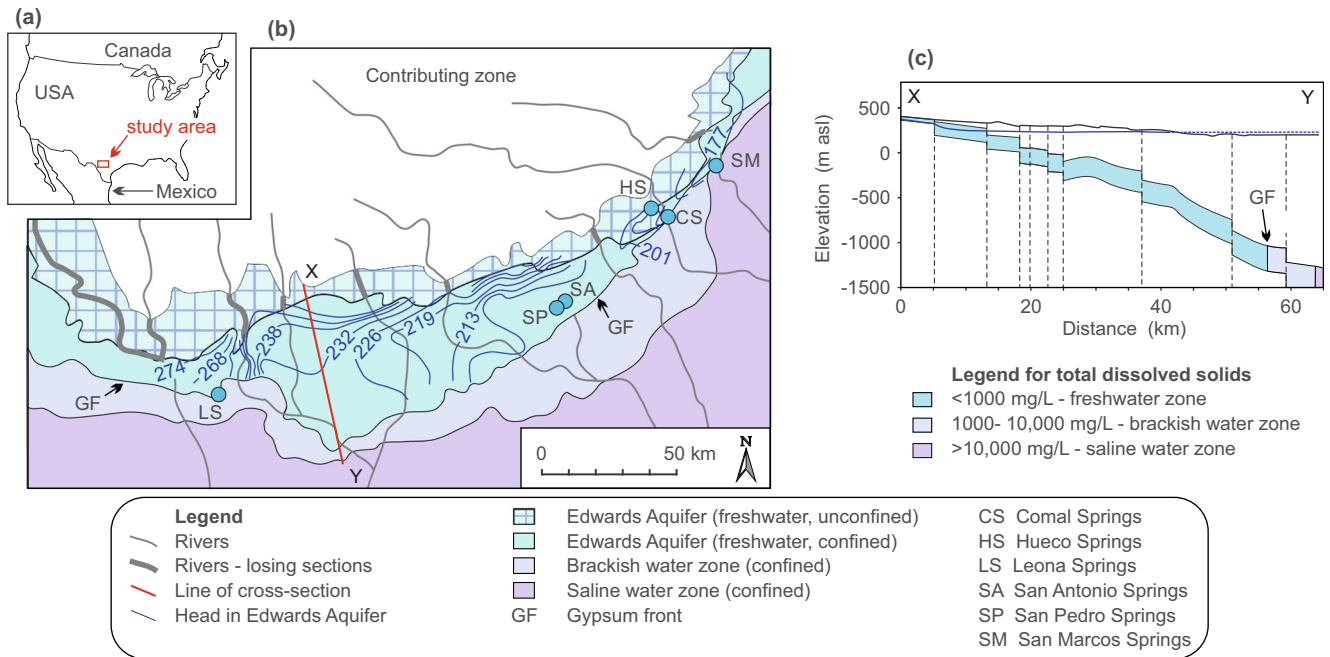
The San Antonio segment of the aquifer is the largest segment, extending for 250 km from a groundwater divide in the west to two major springs in the east, Comal Springs and San Marcos Springs, which have mean discharges of 27 and 16 m^3/s, respectively (Hamilton et al. 2012). A total of 6 m^3/s discharges from Leona, San Pedro, San Antonio, and Hueco springs (Fig. 1). In addition, 40 m^3/s are pumped from wells, giving a total aquifer discharge of 89 m^3/s (Hamilton et al. 2012).

The aquifer dips to the south-east, and the potentiometric surface varies from >250 m above sea level (asl) in the west to 190 m in the east at Comal Springs, and to 174 m at San Marcos Springs (Fig. 1). The zone of freshwater extends downdip in the confined aquifer for as much as 50 km, where the aquifer is more than 1,000 m below the surface (Schindel 2019). At greater depths there is a brackish water zone, where total dissolved solids (TDS) exceed 1,000 mg/L, and further downdip the water become saline, with TDS >10,000 mg/L (Fig. 1). TDS concentrations average 325 mg/L at Comal Springs and 340 mg/L at San Marcos Springs (Hamilton et al. 2012).

Anhydrite beds are almost absent in the freshwater zone of the Edwards Aquifer, but thicken in a zone that is often only several kilometres wide, where TDS rapidly increases from several hundred to several thousand milligrams per litre. Anhydrite beds exceed a thickness of 20 m within a few kilometres of the 1,000 mg/L contour (Schultz and Halty 1997); thus, the 1,000 mg/L contour roughly coincides with the gypsum front. The aquifer is roughly coincident with the Balcones fault zone, an extensive area of normal faults (see section XY in Fig. 1). These date from a period of uplift and faulting in the early Miocene, which marks the start of the modern phase of aquifer development (Sharp and Banner 1997). Since that time, the gypsum front has moved downdip more than 50 km in places such as at section XY in Fig. 1, giving a rate of >2 mm/year.

Deep Geologic Repository, Ontario, Canada

An investigation for a Deep Geologic Repository for nuclear waste in Ontario produced permeability data to depths of 840 m below the surface from packer testing (Al et al. 2011). The site is in Palaeozoic sedimentary rocks on the eastern flank of the Michigan basin, and the strata dip gently to the south-west (Fig. 2). The rocks can be grouped into three principal carbonate aquifers, separated by two aquitards. The Salina Formation forms the upper aquitard, and is composed of a sequence of interbedded halite, gypsum, shale, and carbonate rocks. A thick sequence of Ordovician shales forms the lower aquitard. Precambrian igneous and metamorphic rocks underlie the Palaeozoic sedimentary strata. The unconfined carbonate

Fig. 1 The San Antonio segment of the Edwards Aquifer, showing (**a**) location map, (**b**) plan and (**c**) profile of the aquifer (adapted from Lindgren et al. 2004)

aquifers are widely used for water supplies, and TDS is usually 300–500 mg/L (Singer et al. 2003). The TDS in the carbonate aquifers increases downdip where the aquifers are confined, first to a brackish water zone and then to saline water zone (Fig. 2). Glacial sediments cover almost the whole area, with thicknesses exceeding 100 m in places. Consequently, infiltration is limited, the water table is usually close to the surface, and there is a surface drainage network over the whole area. Groundwater flow in the carbonate formations is largely in local flow systems discharging to rivers, with a component of regional flow discharging directly into Lake Huron.

Arabika aquifer, Abkhazia, Georgia

Cave exploration in the Arabika Massif in the Caucasus Mountains has shown that the water table lies at a depth of 2,145 m below the surface in Krubera Cave (Fig. 3). The strata in the area are composed of Jurassic and Cretaceous limestones that have been subjected to differential uplift during Alpine tectonism. The base of the Cretaceous strata has been uplifted to 200 m asl near the coast, and to >2,000 m asl at the entrance of Krubera Cave, 13 km inland. The unconfined aquifer has been exposed at the surface for some millions of years, and dissolution and cave formation have been ongoing over this
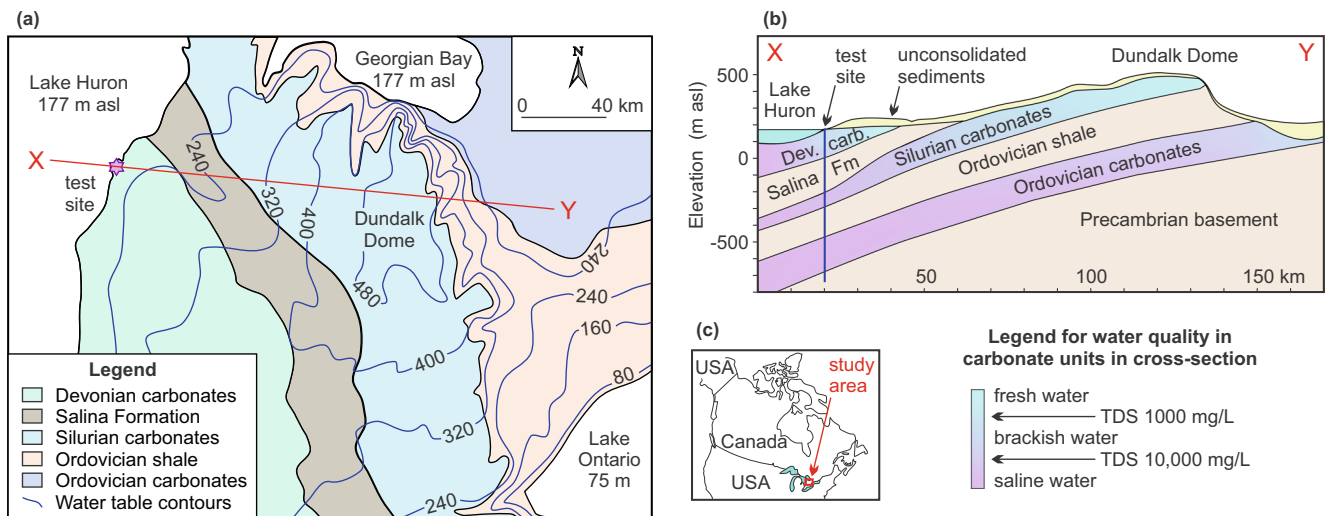
Fig. 2 Plan (**a**) and profile (**b**) of the area of the Ontario Deep Geologic Repository test site (compiled from Singer et al. 2003, Al et al. 2011 and Worthington 2011)

Fig. 3 Profile (**a**) of the Arabika Massif and location map of the area (**b**) (adapted from Klimchouk 2019)
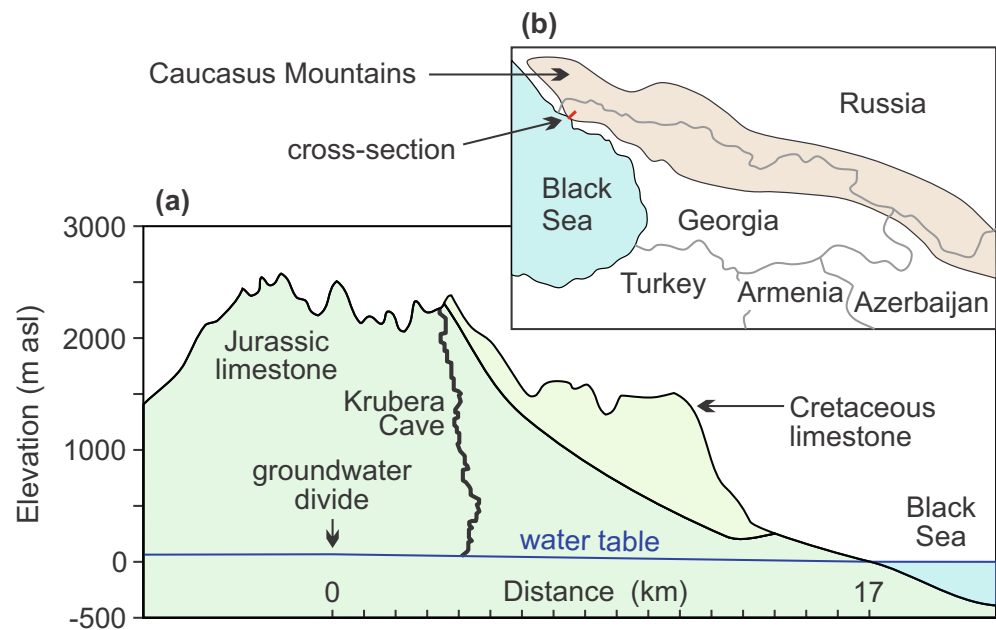
timespan. Consequently, there are likely to have been low water-table gradients similar to those of today over essentially the whole period since the strata were first uplifted above sea level (Klimchouk 2019). Most of the uplift in the Caucasus Mountains has occurred since the late Miocene (Klimchouk 2019). Assuming 2,000 m of uplift in 5 Ma gives an uplift rate of 0.4 mm/year, which may be equated to the rate of downward movement of the base of the freshwater zone in the aquifer.

Chalk aquifer, England, UK

The Chalk is a Cretaceous formation that is extensively exposed in southern and eastern England, where it forms cuestas and plateaus that are generally 100–200 m above sea level (asl). Its porosity averages about 30%, but pore throats are mostly <1 μm (Price 1987). Consequently, little of the matrix porosity drains under gravity, and the specific yield in pumping tests is typically only about 1% (MacDonald and Allen 2001). Chalk aquifers provide about half of the total groundwater use in the UK, and are carefully managed (Lloyd 1993; Shepley et al. 2012). In several areas, the Chalk is pumped in headwaters areas during drought periods, and the water discharged downgradient to the head of perennial sections of streams. Two such areas are shown in Fig. 4, where long-term pumping tests were carried out using multiple wells (Headworth et al. 1982; Connorton and Reed 1978; Morel 1980). Pumping and packer tests, and flowmeter and salt dilution profiling in wells have shown that most flow in the Chalk occurs in solutionally enlarged fractures, typically in the upper 50–60 m of the saturated zone (Price et al. 1982, 1993; Schürch and Buckley 2002; Maurice et al. 2012; Allen and Crane 2019).

Methods

There have been a large number of pumping tests in the Edwards Aquifer that have determined hydraulic conductivity values. However, Halihan et al. (2000) showed that average values from 1,072 pumping tests were about two orders of magnitude lower than is required to calibrate numerical models of the aquifer. This is because pumping test wells are unlikely to be located on the higher-permeability preferential flow paths through carbonate aquifers. Consequently, well-calibrated numerical models give more accurate estimates of aquifer permeability. There have been a number of numerical studies of the aquifer, with recent models having >100,000 cells in the aquifer (Green et al. 2019). The different models have all had similar permeability distributions, and for this study, an early model (Klemt et al. 1979) was used, with a limited number of permeability values that could be more easily plotted. This model was calibrated to water levels in about 100 wells and to spring flows over the period 1947 to 1971.

At the Ontario site, there have been a substantial number of permeability measurements in the uppermost 200 m of strata. Below this depth, data were collected from packer tests in six deep wells (Al et al. 2011). A numerical groundwater model for flow at the site used average hydraulic conductivity values from the packer tests.

In the limestone aquifer in the Caucasus Mountains, there are no deep wells where permeability measurements have been made. However, Haitjema and Mitchell-Bruker (2005) showed that the height of the water table (Δh) above base level can be expressed as
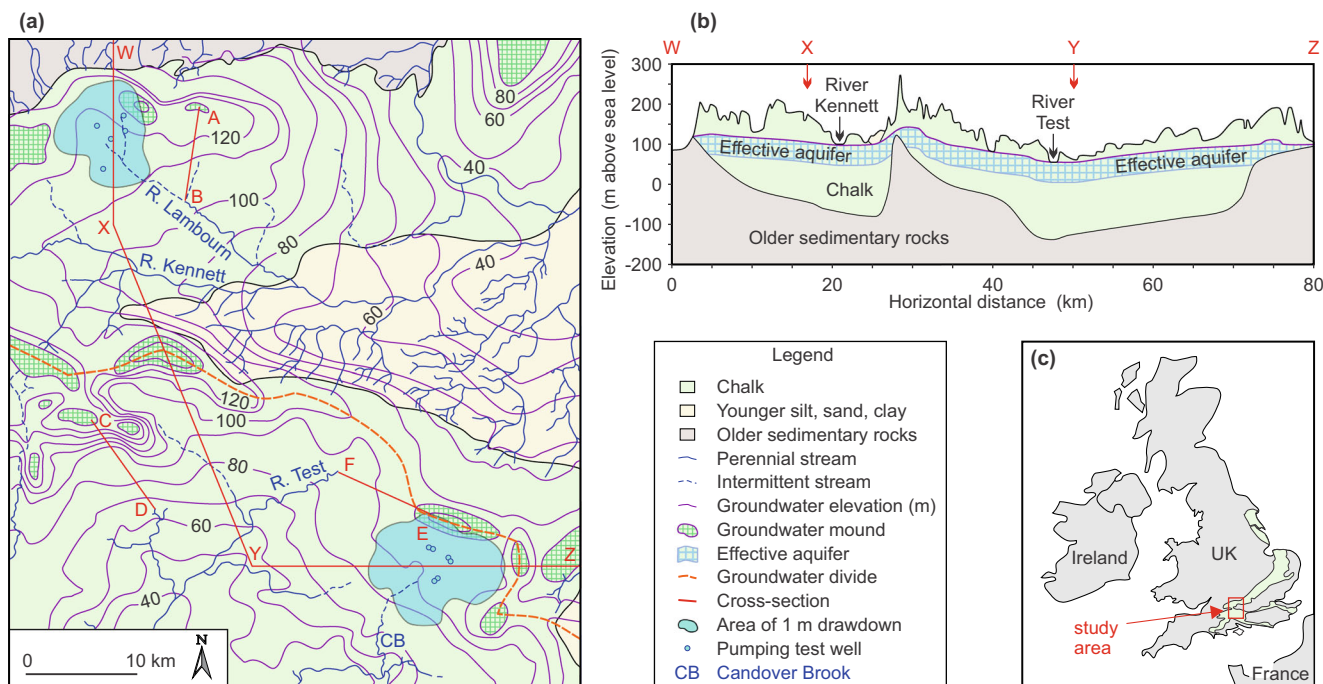
Fig. 4 Plan (**a**), profile (**b**), and location map (**c**) of the Lambourn and Candover pumping tests in the Chalk aquifer (UK), showing drawdown after 90 days of pumping and regional water table elevations (compiled from Institute of Geological Sciences and Thames Water Authority 1978; Institute of Geological Sciences and Southern Water Authority 1979; Owen and Robinson 1978; Headworth et al. 1982)

$$\Delta h = \frac{RL^2}{mKH} \quad (1)$$

where R is aquifer recharge, L is the distance between base level on either side of a mountain range, m is a shape factor which equals 8 in the case of flow from a linear mountain range, K is hydraulic conductivity, and H is aquifer thickness.

The hydraulic conductivity was calculated from Darcy's Law, expressed as $Q = KiA$, where the discharge (Q) is the product of hydraulic conductivity, hydraulic gradient (i), and aquifer cross-section (A). It is assumed that the groundwater divide is 3 km upgradient from Krubera Cave, based on groundwater tracing results (Klimchouk 2019). Tracing has shown that recharge in the area of the cave flows 13 km to a large spring close to the Black Sea coast and at an elevation of 1 m asl (Klimchouk 2019). It is assumed that annual recharge in the mountains is 2,000 mm, diminishing linearly to 1,000 mm at the coast, with a constant 500 mm evapotranspiration. The water table in Krubera Cave is 111 m asl (Klimchouk 2019).

The thickness of the aquifer was calculated from

$$D = 0.18(L\theta)^{0.79} \quad (2)$$

where D is the depth of flow below the water table, L is the flow path length, and θ is the dimensionless dip, equal to the sine of the dip in degrees (Worthington 2001). The equation was developed from 19 cave systems where the maximum depth of flow in cave passages had been determined.

Variation in hydraulic conductivity with depth in the Chalk was derived by two methods. Analysis of the two long-term pumping tests shown in Fig. 4 showed that there was a reduction in transmissivity over time as the water table dropped (Owen and Robinson 1978; Headworth et al. 1982). The data were converted to hydraulic conductivity values as function of depth to facilitate comparison with other areas. The second method was to use calibration results from MODFLOW VKD, which allows hydraulic conductivity and storage to be varied with depth (Water Management Consultants 2002). The Chalk aquifers shown in Fig. 4 have been modelled in a series of regional models—for instance, the area to the west of the River Test is in the Wessex Basin model. This area covers about 2,500 km^2 of the Chalk outcrop, and the model was calibrated to water levels in 284 wells and to river flow over a 40-year period at 42 stations, using three stress periods per month (Soley et al. 2012).
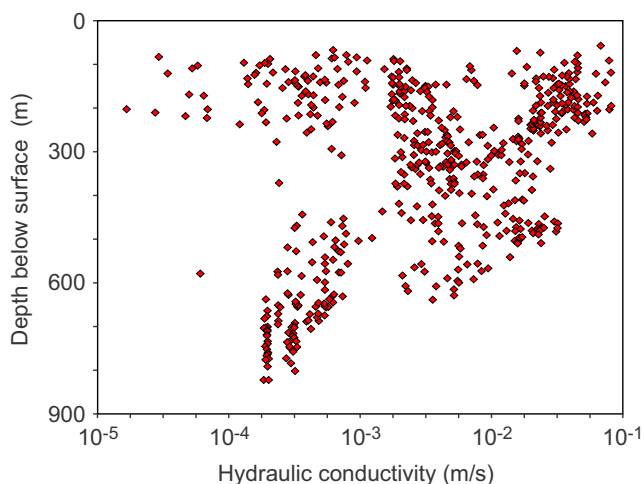
Results

The Klemt et al. (1979) numerical model has hydraulic conductivity values for 546 cells in the freshwater zone of the Edwards Aquifer (Fig. 5). The data are presented as a function of mean aquifer depth at each cell. There are no data for depths below 850 m because the deeper part of the freshwater zone had not been identified when the modelling was carried out. A later model found that the deeper part of the freshwater zone

had similar values to shallower depths, but that values decreased substantially in the brackish water zone, with average values of 4×10^{-6} m/s in that zone (Lindgren et al. 2004). It can be concluded that there is no straightforward trend in hydraulic conductivity with depth in the Edwards Aquifer (Fig. 5).

For the Ontario Deep Geologic Repository, individual packer test results below 200 m are shown in Fig. 6 against the measured test interval. Above 200 m, only average values for each formation are available. There is a clear decrease in hydraulic conductivity from the upper strata (10^{-4}–10^{-7} m/s) to the deeper strata (10^{-7}–10^{-16} m/s), but there is a very wide range in values (Fig. 6). Analysing only the data in the carbonate rocks, there is a rapid increase in TDS with depth, from freshwater near the surface to brines at a depth of 230 m in the Salina Formation (Fig. 6). These are accompanied by low hydraulic conductivity values; however, there are higher values in the carbonate units between –300 and –400 m, with a value $>10^{-7}$ m/s at −330 m coinciding with a low TDS of 28,600 mg/L (Fig. 6). These values occur in the 42-m-thick A1 dolostone unit of the Salina Formation. This provides evidence for downdip flow of freshwater from shallower depths within the Salina A1 dolostone rather than vertical flow through the overlying shale and evaporite aquitards. Further downgradient, flow would continue along the strike, discharging where the Salina A1 dolostone outcrops under Lake Huron. In the deeper carbonates below 500 m, there is no evidence for downdip flow of meteoric water reaching the site, and there are both very low hydraulic conductivity values and very high TDS values (Fig. 6). Overall, there is an inverse correlation between TDS and hydraulic conductivity in the carbonate rocks at the site (Fig. 7).

The hydraulic conductivity for the Arabika Massif was calculated using Eq. 1—Tables S1–S3 of the electronic supplementary material (ESM). The greatest uncertainty in the calculations concerned aquifer thickness. Equation 2 yields an aquifer thickness of 85 m and a resultant hydraulic conductivity of 7×10^{-4} m/s, assuming a constant hydraulic conductivity (Table S1 of the ESM). However, evidence from freshwater in deep wells (Klimchouk 2019) suggests that the aquifer could be much deeper than this. For a thickness of 850 m, the hydraulic conductivity would be 7×10^{-5} m/s (Table S2 of the ESM). Calculations assuming that the hydraulic conductivity is proportional to flow, and hence that the water table has a constant gradient, give a similar mean value of 6×10^{-4} m/s for an 85-m-thick aquifer (Table S3 of the ESM).

In the Candover catchment in the UK Chalk, six abstraction wells 90–120 m deep were pumped for 6 months, with monitoring at nine observation wells within 400 m, and a further 19 observation wells further away (Headworth et al. 1982). The pumping test at the Lambourn site was similar, with five wells pumping simultaneously for 90 days (Owen and Robinson 1978). Hydraulic conductivity was found to diminish with depth at both sites, though the trends are rather different (Fig. 8a). MODFLOW VKD has commonly been used in regional Chalk groundwater models to achieve a satisfactory transient calibration between heads in wells and flow in streams. Transmissivity generally increases in a downgradient direction, from <100 m²/day at interfluves to >1,000 m²/day in valleys (Morel 1980; Soley et al. 2012; Taylor et al. 2012). It has also been found that the depth of enhanced permeability tends to be greater in valleys than at interfluves (Soley et al. 2012). A generalized plot of variation in hydraulic conductivity with depth is shown in Fig. 8b, based on model calibration results in Entec (2007) and Soley et al. (2012). However, locally there are substantial variations from these averages, with Chalk lithology, structure, preferential flow horizons, and preferential recharge all playing a role.
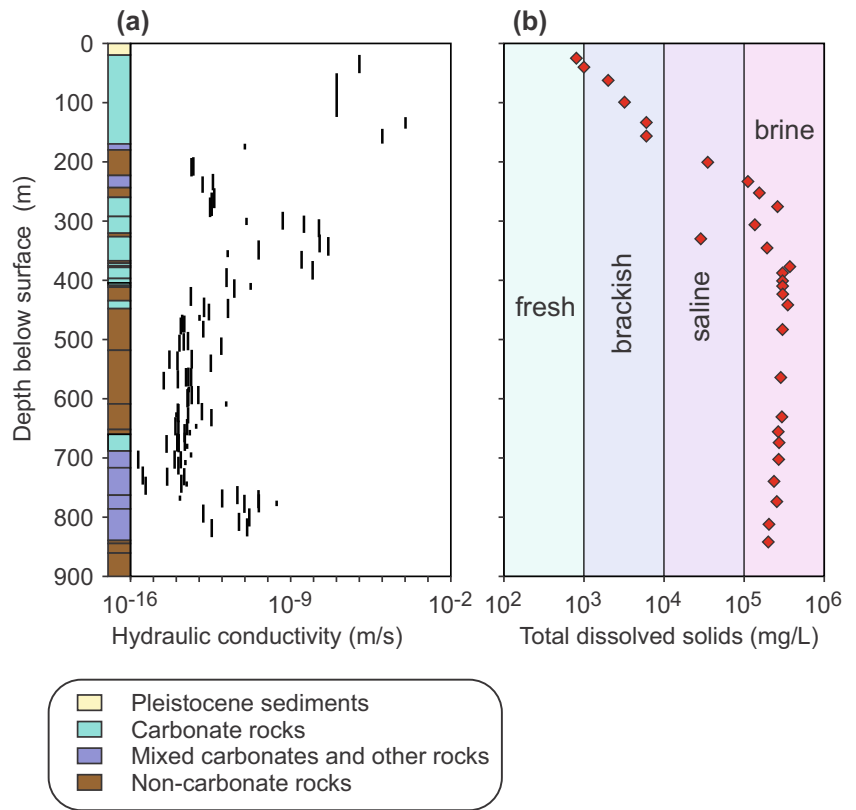
Discussion

The correlation of permeability with depth for the four sites studied is shown in Fig. 9, which also shows the results from Virginia (Sanford 2017). Individual data points are shown as diamonds, and rectangles represent the general range of values for study areas. Results for the UK and for Virginia are represented by general trends. In addition, general trends for the freshwater, brackish water and saline water/brine classes are shown. Overall, the data show substantial scatter and there is no simple trend in either permeability or TDS with depth. The permeability differences shown are influenced by several factors, which are described in the following sections.
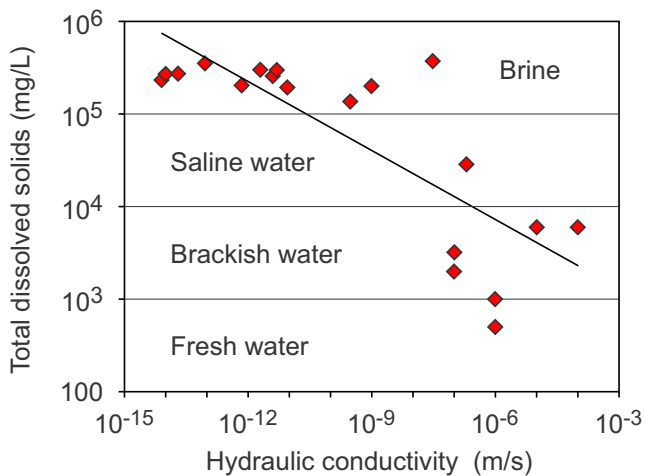
Deep water tables in carbonate mountains

The thick, pure limestones and high rainfall in the Arabika Massif result in substantial dissolution in the

Fig. 5 Hydraulic conductivity as a function of depth in the Edwards Aquifer (based on data in Klemt et al. 1979)

Fig. 6 Profile of hydraulic conductivity (**a**) and total dissolved solids (**b**) at the Ontario Deep Geologic Repository (adapted from Al et al. 2011)

Fig. 7 Correlation of hydraulic conductivity in the carbonate rocks at the Ontario Deep Geologic Repository with total dissolved solids (based on data in Al et al. 2011)

bedrock, which enhances permeability. High infiltration in the limestone and the absence of aquitards results in an absence of surface flow and facilitates the deep infiltration of meteoric water. Following millions of years of uplift there are now high permeabilities together with circulation of freshwater to depths of more than 2,000 m below the surface (Fig. 3). The hydraulic conductivity of near-surface carbonate rocks globally is on average 2×10^{-5} m/s, and is substantially higher than in other lithologies

(Gleeson et al. 2011). Calculations using Eq. (1) have shown that the low hydraulic gradients in the Arabika Range necessitate similarly high hydraulic conductivities (Fig. 9).

The occurrence of deep water tables and the presence of freshwater at great depths are common in mountains that have thick sequences of carbonate rocks. The existence of many deep caves around the world attests to this (Gulden 2020). Well-documented examples where caves have been explored to depths >1,000 m and where the water table is <100 m above spring elevation include the Picos de Europa in Spain (Ballesteros et al. 2015) and the Velebit Mountains in Croatia (Stroj and Paar 2019). In both these cases there are low hydraulic gradients and so high hydraulic conductivities similar to the aquifer at Krubera Cave.

Inhibited vertical flow due to aquitards

The presence of aquitards in carbonate sequences can limit vertical flow of recharge water and hence limit dissolutional increases in permeability. The examples from Canada and from Georgia provide examples of the contrasts. At the Canadian Deep Geologic Repository site, there are widespread unconsolidated sediments with varied permeability, and substantial surface flow in rivers. The bedrock consists of interbedded carbonates and lower-permeability rocks, including shale, gypsum, and halite. These factors limit the ingress of meteoric water,

Fig. 8 Profiles of hydraulic conductivity as a function of depth below the water table in the Chalk aquifer, UK, with data from long-term pumping tests (**a**) and from model calibration (**b**). Calculated from data in Owen and Robinson (1978), Headworth et al. (1982), Entec (2007), and Soley et al. (2012)
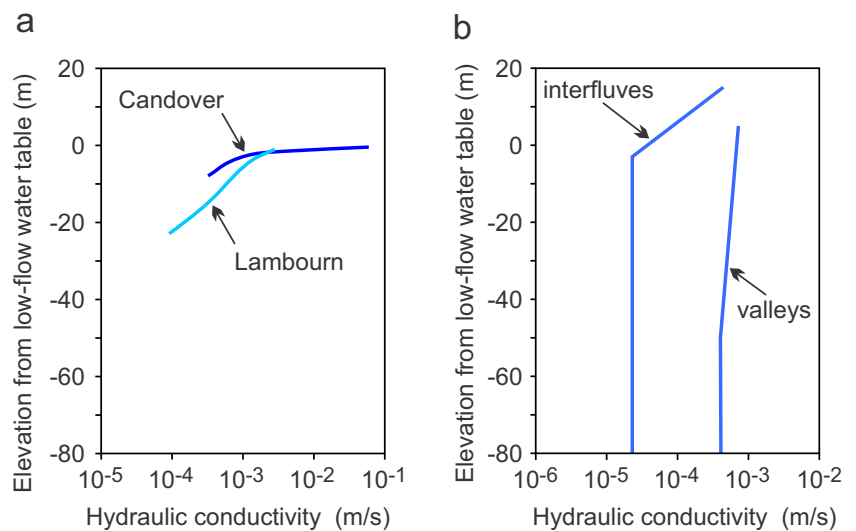
especially below a depth of 220 m, where brines predominate and the permeability is very low (Fig. 9). The Arabika aquifer in Georgia lacks aquitards and has much higher permeability at depth than the Canadian site (Fig. 9).

Chemical undersaturation and the flowrate effect

Solutional enlargement of fractures incorporating the nonlinear dissolution kinetics of calcite is a function of a number of factors. These include fracture aperture, initial partial pressure of CO_2 of recharge water, hydraulic gradient, flow path length, and the changing chemical undersaturation with respect to Ca along the flow path (Dreybrodt 1990; Palmer 1991). For an unconfined aquifer with infiltration over the whole aquifer, application of Darcy's law shows that initial

hydraulic gradients increase in a downgradient direction. Consequently, steep gradients and short flow paths will favour more dissolution in the downgradient part of the aquifer, but greater chemical undersaturation will favour more dissolution in the upgradient part of the aquifer if there is substantial chemically-undersaturated sinking-stream recharge. Liedl et al. (2003) examined these competing factors and showed that dissolution commonly results in greater enlargement in downgradient fractures, with the water table evolving from an initial convex shape to a later concave shape. Furthermore, the development of a concave water table is also enhanced by mixing dissolution and by the earlier transition to turbulent flow in downgradient parts of the aquifer where there is more flow (Romanov et al. 2003; Kaufmann 2016). The development of a concave water table is largely a function of the

Fig. 9 Relationship between hydraulic conductivity, depth and total dissolved solids in carbonate rocks in the Ontario, Georgia, UK, and two US (Texas and Virginia) aquifers (based on data in Klemt et al. 1979, Entec 2007, Al et al. 2011, Sanford 2017, and Klimchouk 2019). Diamonds refer to data points; rectangles indicate the general range of values for study areas
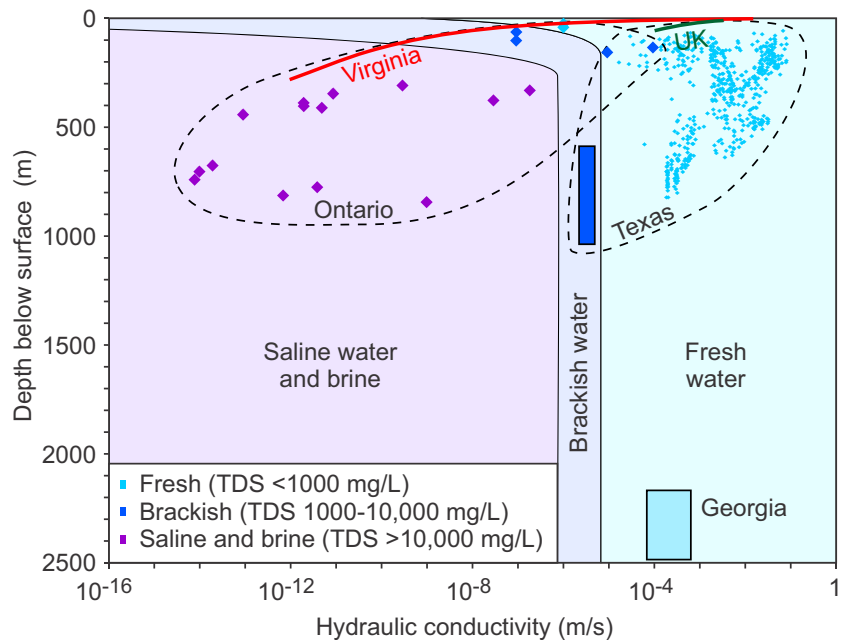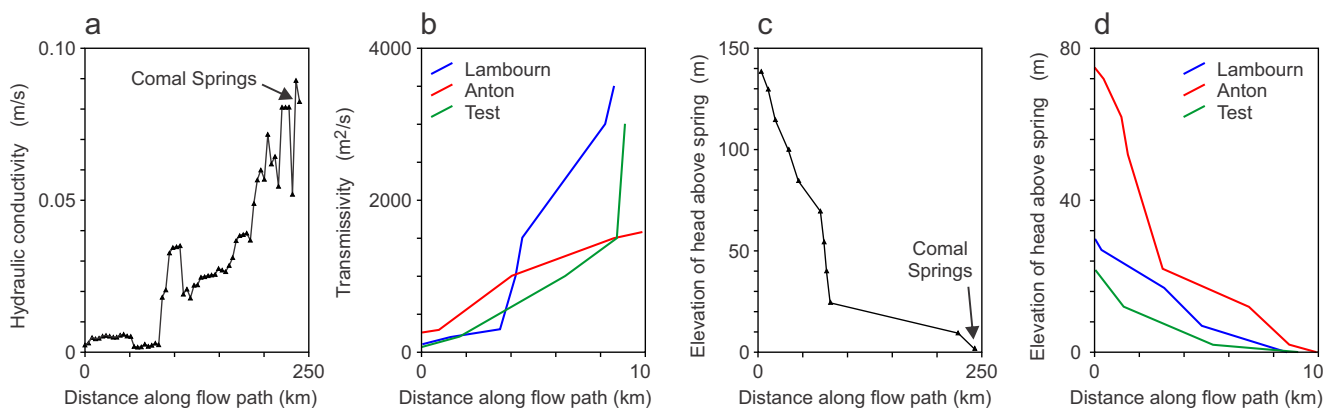
Fig. 10 Trends of hydraulic conductivity and transmissivity in a downgradient direction (**a**–**b**), and decreasing hydraulic gradient in a downgradient direction (**c**–**d**) in the confined aquifer on the main flow path to Comal Springs (**a** and **c**) and along three flow paths in the UK Chalk (**b** and **d**) (based on data from Klemt et al. 1979; Lindgren et al. 2004; Power and Soley 2004). The three flow paths in the Chalk are shown in Fig. 4

increasing permeability in a downgradient direction being associated with increased flow, so this effect is described here as the flowrate effect.

The concave shape of the water table in carbonate aquifers and its association with sinking streams and springs was demonstrated by mapping of the water table over an area of 1,600 km^2 in Kentucky, USA (Quinlan and Ewers 1989). Water levels from 1,500 wells and from cave streams in 700 km of caves were used, together with results from 500 tracer tests. The mapping showed how the major flow paths are along groundwater troughs linking sinking streams to springs, with gradients decreasing in a downgradient direction (Quinlan and Ewers 1989). A numerical model of one of the major groundwater basins showed that hydraulic conductivity increases by one to three orders of magnitude between sinking streams and springs (Worthington 2009).

In the Chalk aquifer, there are substantial downgradient decreases in hydraulic gradients, giving concave profiles (Fig. 1); thus, the steepest hydraulic gradients in the Chalk do not occur in downgradient locations proximal to streams, as would occur in an aquifer with uniform permeability. Instead, the steepest hydraulic gradients occur in upgradient locations on the perimeters of groundwater mounds, where the permeability is low. This is clearly seen in Fig. 4, on the margins of the 14 groundwater mounds which are located on interfluves. Figure 10 shows downgradient trends in the Edwards aquifer to Comal Springs, the largest springs, and in the Chalk aquifer to springs at the perennial heads of the rivers Lambourn, Anton, and Test. The trends in hydraulic conductivity and hydraulic gradient are similar in Texas and the Chalk (Fig. 10). In the former case most of the aquifer recharge is via sinking streams and in the latter case <1% of aquifer recharge is from sinking streams. Thus, preferential flow and substantial downgradient increases in permeability occur not only where there is substantial sinking stream recharge, but also where recharge is by diffuse infiltration.

These trends show the importance of the flowrate effect, where downgradient increases in flow are associated with large downgradient increases in hydraulic conductivity. In addition, the flowrate effect is also significant in a vertical sense. Most flow in the three aquifers studied takes place in the freshwater zones, and it is in these zones that most dissolutional enhancement of permeability has taken place (Fig. 9).

Conclusion

The concept of weathering zones helps give a broad perspective on the flow and weathering processes occurring in aquifers. The analysis here has shown that high permeability in the four carbonate aquifers studied is limited to the freshwater zone. However, the depth of this zone can vary widely, from 40 m at the Ontario site to in excess of 2,000 m in the Caucasus Mountains in Georgia. These differences are due to both stratigraphy and structure. A shallow freshwater zone is favoured in carbonate rocks where they are interbedded with aquitards such as shale. In addition, low stratal dips favour shallow weathering zones. Conversely, deep weathering zones are favoured where there are thick sequences of pure carbonates, especially in mountain ranges where deep vadose zones can develop. They are also favoured where stratal dips are high enough to facilitate flow along the strike of the strata to springs at lower elevations. Weathering fronts can advance at rates of several millimetres per year over periods of millions of years, as in the case of the gypsum front in the Edwards Aquifer.

Total dissolved solids (TDS) concentrations have an inverse correlation with permeability because aquifer permeability is a function of the volume of water that has passed through a carbonate aquifer since substantial groundwater flow started. Low permeabilities in brackish water, saltwater, and brine zones are due to the limited groundwater flow and the associated limited solutional enhancement of permeability. Higher

permeabilities are associated with freshwater zones, where large volumes of meteoric water have flowed through aquifers, and the concomitant dissolution along preferential flow paths such as fractures has greatly enhanced permeability.

References

Al T, Beauheim R, Crowe R, Diederichs M, Frizzell R, Kennell L, Lam T, Parmenter A, Semec B (2011) Geosynthesis: OPG's Deep Geological Repository for low & intermediate level waste. Report NWMO DGR-TR-2011-11, Nuclear Waste Management Organization, Toronto

Allen DJ, Crane EJ (2019) The Chalk aquifer of the Wessex Basin. Research report RR/11/02, British Geological Survey, Nottingham, UK

Anderson MP (2008) Groundwater. Benchmark Papers in Hydrology, no. 3. International Association of Hydrological Sciences, Wallingford, UK, 625 pp

Ballesteros D, Malard A, Jeannin PY, Jiménez-Sánchez M, García-Sansegundo J, Meléndez-Asensio M, Sendra G (2015) KARSYS hydrogeological 3D modeling of alpine karst aquifers developed in geologically complex areas: Picos de Europa National Park (Spain). Environ Earth Sci 74:7699–7714

Berner EK, Berner RA (2012) Global environment. Princeton University Press, Princeton, NJ

Brantley SL, Holleran ME, Jin L, Bazilevskaya E (2013) Probing deep weathering in the Shale Hills critical zone observatory, Pennsylvania (USA): the hypothesis of nested chemical reaction fronts in the subsurface. Earth Surf Processes Landforms 38:1280–1298

Brantley SL, Lebedeva MI, Balashov VN, Singha K, Sullivan PL, Stinchcomb G (2017) Toward a conceptual model relating chemical reaction fronts to water flow paths in hills. Geomorphology 277:100–117

Connorton BJ, Reed RN (1978) A numerical model for the prediction of long term well yield in an unconfined chalk aquifer. Q J Eng Geol Hydrogeol 11:127–138

Domenico PA (1972) Concepts and models in groundwater hydrology. McGraw-Hill, New York

Dreybrodt W (1990) The role of dissolution kinetics in the development of karst aquifers in limestone: a model simulation of karst evolution. J Geol 98:639–655

Ehrenberg SN, Nadeau PH (2005) Sandstone vs. carbonate petroleum reservoirs: a global perspective on porosity-depth and porosity-permeability relationships. AAPG Bull 89:435–445

Entec (2007) East Hampshire and Chichester chalk numerical modelling project, phase 2A: model construction and refinement. Environment Agency, Southern Region, Bristol, UK

Ford DC, Williams PW (2007) Karst hydrogeology and geomorphology. Wiley, Chichester, UK, 562 pp

Freeze RA, Cherry JA (1979) Groundwater. Prentice-Hall, Englewood Cliffs, NJ

Gleeson T, Smith L, Moosdorf N, Hartmann J, Dürr HH, Manning AH, van Beek LPH, Jellinek AM (2011) Mapping permeability over the surface of the earth. Geophys Res Lett 46:L02401. https://doi.org/10.1029/2010GL045565

Goldich SS (1938) A study in rock-weathering. J Geol 46:17–58

Green RT, Winterle J, Fratesi B (2019) Numerical groundwater models for Edwards aquifer systems. In: Sharp JM Jr, Green RT, Schindel GM (eds) The Edwards aquifer: the past, present, and future of a vital water resource. Geol Soc Am Mem 215:19–28

Gulden B (2020) World's deepest caves. http://www.caverbob.com/wdeep.htm. Accessed 8 August 2020

Haitjema HM, Mitchell-Bruker S (2005) Are water tables a subdued replica of the topography? Groundwater 43:781–786

Halihan T, Sharp JM, Mace RE (2000) Flow in the San Antonio segment of the Edwards aquifer: matrix, fractures, or conduits? In: Sasowsky ID, Wicks CM (eds) Groundwater flow and contaminant transport in carbonate aquifers. Balkema, Rotterdam, The Netherlands, pp 129–146

Hamilton JM, Johnson S, Esquilin R, Burgoon C, Luevano G, Gregory D, Mireles J, Gloyd R, Schindel GM (2012) Edwards aquifer authority hydrologic data report for 2011. Edwards Aquifer Authority, San Antonio, TX

Headworth HG, Keating T, Packman MJ (1982) Evidence for a shallow highly-permeable zone in the Chalk of Hampshire, UK. J Hydrol 55:93–112

Hovorka SD, Dutton AR, Ruppel SC, Yeh JS (1996) Edwards aquifer ground-water resources: geologic controls on porosity development in platform carbonates, South Texas. Report of investigations no. 238, Bureau of Economic Geology, University of Texas at Austin, Austin, TX

Hovorka SD, Mace RE, Collins EW (1998) Permeability structure of the Edwards aquifer, South Texas: implications for aquifer management. Report of investigations no. 250, Bureau of Economic Geology, University of Texas at Austin, Austin, TX

Hubbert MK (1940) The theory of groundwater motion. J Geol 48:785–944

Ingebritsen S, Gleeson T (2017) Crustal permeability. Hydrogeol J 25:2221–2224

Institute of Geological Sciences and Thames Water Authority (1978) Hydrogeological map of the South West Chilterns and the Berkshire and Marlborough Downs, 1:100,000. British Geological Survey, Keyworth, UK

Institute of Geological Sciences and Southern Water Authority (1979) Hydrogeological map of Hampshire and the Isle of Wight, 1:100,000. British Geological Survey, Keyworth, UK

Jeannin PY (2001) Modeling flow in phreatic and epiphreatic karst conduits in the Hölloch Cave (Muotatal, Switzerland). Water Resour Res 37:191–200

Kaufmann G (2016) Modelling karst aquifer evolution in fractured, porous rocks. J Hydrol 543:796–807

Klemt WB, Knowles TR, Edler GR, Sieh TW (1979) Ground-water resources and model applications for the Edwards (Balcones Fault Zone) Aquifer in the San Antonio Region. Texas Water Development Board Report 239, TWDB, Austin, TX, 88 pp

Klimchouk A (2019) Krubera (Voronja) Cave. In: White WB, Culver DC, Pipan T (eds) Encyclopedia of caves. Academic, London, pp 627–634

Kresic N (2013) Water in karst: management, vulnerability, and restoration. McGraw-Hill, New York, 708 pp

Lachassagne P, Wyns R, Dewandel B (2011) The fracture permeability of hard rock aquifers is due neither to tectonics, not to unloading, but to weathering processes. Terra Nova 23:145–161

LeGrand HE, Stringfield VT (1971) Development and distribution of permeability in carbonate aquifers. Water Resour Res 7:1284–1294

Liedl R, Sauter M, Hückinghaus D, Clemens T, Teutsch G (2003) Simulation of the development of karst aquifers using a coupled continuum pipe flow model. Water Resour Res 39(3):1057. https://doi.org/10.1029/2001WR001206

Lindgren RJ, Dutton AR, Hovorka SD, Worthington SRH, Painter SC (2004) Conceptualization and simulation of the Edwards aquifer, San Antonio region, Texas. US Geol Surv Sci Invest Rep 2004-5277

Lloyd JW (1993) The United Kingdom. In: Downing RA, Price M, Jones GP (eds) The hydrogeology of the Chalk of North-West Europe. Clarendon, Oxford, pp 220–249

Manning CE, Ingebritsen SE (1999) Permeability of the continental crust: implications of geothermal data and metamorphic systems. Rev Geophys 37:127–150

MacDonald AM, Allen DJ (2001) Aquifer properties of the Chalk of England. Q J Eng Geol Hydrogeol 34:371–384

Maurice LD, Atkinson TC, Barker JA, Williams AT, Gallagher AJ (2012) The nature and distribution of flowing features in a weakly karstified porous limestone aquifer. J Hydrol 438–439:3–15

Milanović PT (1981) Karst hydrogeology. Water Resource Publications, Littleton, CO 434 p

Morel EH (1980) The use of a numerical model in the management of the Chalk aquifer in the upper Thames Basin. Q J Eng Geol 13:153–165

Owen M, Robinson VK (1978) Characteristics and yield in fissured chalk. In: Thames groundwater scheme. Institution of Civil Engineers, London, pp 33–49

Palmer AN (1991) Origin and morphology of limestone caves. Geol Soc Am Bull 103:1–21

Palmer AN (2007) Cave geology. Cave Books, Dayton, OH, 454 pp

Phillips JD, Pawlik Ł, Šamonil P (2019) Weathering fronts. Earth-Sci Rev 198:102925

Power T, Soley R (2004) A comparison of chalk groundwater models in and around the river test catchment. Environment Agency, London

Price M (1987) Fluid flow in the Chalk of England. In: Goff JC, Williams BPJ (eds) Fluid flow in sedimentary basins and aquifers. Geol Soc Spec Publ 34:141–156

Price M, Morris B, Robertson A (1982) A study of intergranular and fissure permeability in chalk and Permian aquifers, using double packer injection testing. J Hydrol 54:401–423

Price M, Downing RA, Edmunds WM (1993) The Chalk as an aquifer. In: Downing RA, Price M, Jones GP (eds) The hydrogeology of the Chalk of North-West Europe. Clarendon, Oxford, pp 33–58

Quinlan JF, Ewers RO (1989) Subsurface drainage in the mammoth cave area. In: White WB, White EL (eds) Karst hydrology: concepts from the mammoth cave area. Van Nostrand Reinhold, New York, pp 65–103

Ranjram M, Gleeson T, Luijendijk E (2015) Is the permeability of crystalline rock in the shallow crust related to depth, lithology or tectonic setting? Geofluids 15:106–119

Romanov D, Gabrovsek F, Dreybrodt W (2003) The impact of hydrochemical boundary conditions on the evolution of limestone karst aquifers. J Hydrol 276:240–253

Sanford WE (2017) Estimating regional-scale permeability–depth relations in a fractured-rock terrain using groundwater-flow model calibration. Hydrogeol J 25:405–419

Schindel GM (2019) Genesis of the Edwards (Balcones fault zone) aquifer. In: Sharp JM Jr, Green RT, Schindel GM (eds) The Edwards aquifer: the past, present, and future of a vital water resource. Geol Soc Am Mem 215

Schultz AL, Halty SR (1997) Anhydrite: source of high sulfate concentration near Edwards aquifer "bad-water" line. Bull South Texas Geol Soc 37:11–16

Schürch M, Buckley D (2002) Integrating geophysical and hydrochemical borehole-log measurements to characterize the Chalk aquifer, Berkshire, United Kingdom. Hydrogeol J 10:610–627

Sharp JM, Banner JL (1997) The Edwards aquifer: a resource in conflict. GSA Today 7(8):1–9

Sharp JM Jr, Green RT, Schindel GM (eds) (2019) The Edwards aquifer: the past, present, and future of a vital water resource. Geol Soc Am Mem 215

Shepley MG, Whiteman MI, Hulme PJ, Grout MW (2012) Groundwater resources modelling: a case study from the UK. Geol Soc London Spec Publ 364

Singer SN, Cheng CK, Scafe MG (2003) The hydrogeology of southern Ontario. Environmental Monitoring and Reporting Branch, Ministry of the Environment, Ottawa

Soley RWN, Power T, Mortimore RN, Shaw P, Dottridge J, Bryan G, Colley I (2012) Modelling the hydrogeology and managed aquifer system of the Chalk across southern England, London. Geol Soc Spec Publ 234:129–154

Stringfield VT, Le Grand HE (1966) Hydrology of limestone terranes in the Coastal Plain of the southeastern United States. Geol Soc Am Spec Pap 93

Stevanović Z (2015) Karst aquifers: characterization and engineering. Springer, Cham, Switzerland, 692 pp

Stroj A, Paar D (2019) Water and air dynamics within a deep vadose zone of a karst massif: observations from the Lukina jama–Trojama cave system (–1,431 m) in Dinaric karst (Croatia). Hydrol Proc 33:551–561

Taylor AB, Martin NA, Everard E, Kelly TJ (2012) Modelling the Vale of St Albans: parameter estimation and dual storage. Geol Soc London Spec Publ 364:193–204

Water Management Consultants (2002) Enhancements to MODFLOW: variations in hydraulic conductivity and storage with depth. NGCLC Project NC/00/23, Environment Agency, London

Worthington SRH (2001) Depth of conduit flow in unconfined carbonate aquifers. Geology 29:335–338

Worthington SRH (2009) Diagnostic hydrogeologic characteristics of a karst aquifer (Kentucky, USA). Hydrogeol J 17:1665–1678

Worthington SRH (2011) Karst assessment: OPG's Deep Geological Repository for low & intermediate level waste. Report NWMO DGR-TR-2011-22, Nuclear Waste Management Organization, Toronto

Worthington SRH, Ford DC (1995) High sulfate concentrations in limestone springs: an important factor in conduit initiation? Environ Geol 25:9–15

Worthington SRH, Ford DC (2009) Self-organized permeability in carbonate aquifers. Groundwater 47:326–336

Worthington SRH, Davies GJ, Alexander EC Jr (2016) Enhancement of bedrock permeability by weathering. Earth-Sci Rev 160:188–202